

Polarization-sensitive optical coherence tomography of invasive basal cell carcinoma

John Strasswimmer, MD, PhD

Mark C. Pierce, PhD

B. Hyle Park, MSc

Victor Neel, MD, PhD

Johannes F. de Boer, PhD

Wellman Center of Photomedicine

Department of Dermatology

Massachusetts General Hospital

Harvard Medical School

50 Blossom Street

Boston, Massachusetts 02114

Abstract. Skin cancer is the most common human malignancy, with basal cell carcinoma (BCC) the most frequent type. Aggressive forms of BCC are associated with extensive dermal invasion and destruction of collagen. Surgery is the most common treatment, but identification of tumor borders is a challenge. Polarization-sensitive optical coherence tomography (PS-OCT) is an optical method to examine collagen birefringence. To date, it has not been exploited for cancer management. As part of a pilot exploratory study to examine the use of OCT in skin cancer, we examined several tumors that pose a challenge to the surgeon due to their large size and histological subtype. In normal perilesional skin, OCT identifies epidermal and dermal structure; PS-OCT identified dermal birefringence. In BCC, tumors lost normal structure and gained the appearance of lobular impressions. PS-OCT identified an alteration of dermal birefringence. Examination of a border area revealed a gradual transition from more normal appearing image to frank tumor. These results indicate that PS-OCT can identify features that distinguish normal skin from tumor and may have the potential to guide surgeons in the treatment of aggressive skin cancer.

© 2004 Society of Photo-Optical Instrumentation Engineers. [DOI: 10.1117/1.1644118]

Keywords: basal cell carcinoma; optical coherence tomography; birefringence; collagen.

Paper 014014 received Apr. 16, 2003; revised manuscript received Jun. 30, 2003; accepted for publication Jun. 30, 2003.

1 Introduction

Basal cell carcinoma (BCC) is the most common human malignancy, with an incidence of nearly one million per year in the United States. The reader is referred to a comprehensive review of the biology of this tumor.¹ Currently, diagnosis requires invasive biopsy. In addition to the pain, expense, and scarring of the actual biopsy procedure, approximately 20% of biopsies misidentify aggressive subtypes of tumor² due to sampling error. Noninvasive diagnosis methods have the potential to address these limitations and allow the clinician to assess lesions during treatments and monitor for recurrence. This is of particular importance in the case of aggressive types of BCC, which are either greater than 2.0 cm in diameter or of the infiltrative or morpheaform histological subtypes. In these cases, large surgical margins are taken in order to ensure complete tumor extirpation, leading to unnecessary removal of healthy tissue. Mohs micrographic surgery relies on a series of frozen tissue sections and interpretation by the surgeon. This increases the cost and the time the patient has an open wound. This technique is only available to specially trained dermatologic surgeons. Therefore, a method that might guide the surgeon to identify tumor borders would be a significant clinical aid.

Several technologies have been explored as possible non-invasive diagnostic methods. However, they suffer from prac-

tical limitations. High-frequency ultrasound,³ terahertz imaging,⁴ and magnetic resonance⁵ offer insufficient resolution at this time. Reflectance confocal microscopy (RCM) produces high-quality images of BCC.⁶ It is encumbered by the small field of examination, limited depths of imaging, and the mirror-based design. None of these methods has been exploited for invasive tumor demarcation.

Optical coherence tomography (OCT) combines high resolution with good tissue penetration. Cutaneous structure, including the entire epidermis, a portion of the dermis, and appendages can be identified (Pierce et al.¹⁷). Recent modifications of OCT promise to expand the utility of OCT. Doppler sensitivity (optical Doppler tomography) has been exploited to evaluate treatment of a vascular lesion.⁷ Polarization-sensitive OCT (PS-OCT) takes advantage of the polarization information carried by light to identify tissue birefringence.⁸ In skin, birefringence is attributed to the regular arrangement of collagen fibers in the dermis. PS-OCT allows polarization effects to be quantified and related to the structural integrity of the collagen scaffold, as demonstrated by PS-OCT imaging of thermally damaged skin.⁹ In addition to the thermally induced changes in dermal birefringence, there is marked variability in the birefringence of human skin *in vivo*¹⁷ and therefore any method must be able to rapidly measure local variations and compare them with localized disease processes.

Basal cell carcinomas are characterized by their local invasion caused by several mechanisms.¹ As they progress

Address correspondence to John Strasswimmer. Tel: 617-724-2257; Fax: 617-726-4103; E-mail: jstrasswimmer@PARTNERS.ORG

Address correspondence also to Johannes de Boer. Tel: 617-724-2202; Fax: 617-726-4103; E-mail: jdeboer@PARTNERS.ORG

deeper into the skin, the normal architecture is lost, including the adnexae (vessels, pilosebaceous units, nerves, and glands). This is attributed to action of proteases released from the tumor cells and altered collagen synthesis by tumor stromal cells. In addition to the altered collagen, the tumors are characterized by retraction gaps filled with mucopolysaccharides (MPS). The combination of loss of normal adnexal structures, destruction of collagen, synthesis of MPS alters the fundamental structure of the dermis.

Initial attempts to use OCT for BCC characterization were disappointing, due to limited resolution, imaging depth, and speed.¹⁰ Improvements in the OCT technique, including the ability to acquire, process, and display in real time, with improved optical design, along with the addition of polarization sensitivity revealed that one can reliably measure dermal birefringence and acquire important architectural information about normal skin.¹⁷ Because of the alterations in dermis associated with BCC, we examined whether PS-OCT can distinguish tumor from surrounding uninvolved skin.

2 Methods

2.1 Clinical Study

We designed a pilot, noninvasive, exploratory study of the potential for PS-OCT to identify features of BCC. Volunteers were recruited from the Dermatology Department of the Massachusetts General Hospital under a protocol approved by the Partners Human Research Committee. Volunteers had a diagnosis of basal carcinoma confirmed by biopsy of a portion of the lesion as part of their routine medical care. Prior to definitive surgery by excision or by Mohs micrographic surgery, OCT images were acquired in different portions of the tumor, border area, and of adjacent uninvolved skin. The system was set up to acquire scans measuring 5 mm wide and 1.2 mm deep. Imaging was performed with the application of water or glycerol directly on the skin and direct contact with the glass plate of the OCT handpiece or with a thin medical transparent film (Tegaderm, 3M, Inc.). Subsequently, the regions scanned by OCT were compared to representative histology of the region to ensure that they corresponded to tumor, normal skin, or border region. As this was a pilot, noninvasive study, no attempt was made to mark the specimen *in situ* prior to the surgery or to obtain exact alignment of the OCT and histological sections.

2.2 OCT Instrumentation

The details of the PC-OCT system used in this study have been reported in detail elsewhere.¹⁶ Briefly, a semiconductor optical amplifier is employed as the light source, with a bandwidth of 70 nm centered at a wavelength of 1310 nm. Light is passed to the skin through a fiber-optic system to a lightweight handpiece, resulting in a power of 7 mW incident on the skin, focused to a spot size of 30 μm . This power level is below the safe occupational exposure level established by the American National Standards Institute (ANSI Z136.1). The infrared light source used for OCT imaging cannot be seen by the eye; therefore a visible beam at 630 nm is coupled through the system, enabling the user to directly identify the scanned location in real time.

Light is backscattered from the skin and recombined with a control beam from a reference mirror and divided between

two detectors for orthogonal polarization states. Signals at both detectors are amplified, filtered, and digitized before all subsequent data processing and display are performed in software. Conventional OCT images of backscattered light intensity are generated by displaying the amplitude of the interference fringe envelope, which is subsequently mapped onto an 8-bit gray scale. Black represents high backscattering intensity.

Polarization-sensitive OCT images identify birefringent tissue regions by measuring depth-resolved changes in the polarization state of light reflected from tissue that produce a phase retardation angle Φ . In our images, we display the intensity-weighted mean of the phase retardation angles experienced by the two incident polarization states of light on a gray scale from black (0°) to white (180°), and cycling back to black again for a full wave retardation (360°). The rate at which the polarization state of light changes with depth is proportional to the magnitude of tissue birefringence, which may be visualized by the frequency of black to white transitions in polarization-sensitive images. After light has undergone multiple scattering events, the polarization state is lost and appears in the image as a scrambled signal.

It should however, be noted that both intensity OCT and PS-OCT images are obtained from data acquired in a single B scan, and real-time display is achieved by updating images 32 times each second in a continuously scrolling manner. All image sets presented here were acquired and displayed simultaneously in less than 1 s. Images were not processed in any way beyond that created by the OCT system itself. Plots of the phase retardation per micron of tissue depth were calculated as described previously.⁹

3 Results

As part of a larger case series to evaluate the potential for OCT to aid in management of cutaneous tumors, we examined a set of invasive tumors to determine if alterations in dermal birefringence were identifiable by PS-OCT. Large, aggressive tumors are the most clinically challenging;¹¹ an optical method might have the potential to guide the surgeon. Aggressive BCC types vary from nodular lesions, which frequently ulcerate and produce near-complete replacement of dermis with tumor, to infiltrative types, which more subtly grow deep in the tissue leaving partially intact epidermis and dermis.¹² Representative results for two aggressive types of tumor are presented in this study, and the clinical images for both are presented in Fig. 1. In the first case, a 76-year-old patient presented with a large ulcerated basal cell carcinoma of the nodular and infiltrative subtype (Fig. 1A). Nodular BCCs are characterized by large island "lobules" of tumor that grow from the epidermis into the dermis, as the histopathology specimen reveals (Fig. 1C). An area representing uninvolved perilesional skin was identified 1.5 cm from the nearest clinically apparent tumor margin. This area was selected in order to control for factors which alter the usual skin structure: regional variations in epidermal and dermal thickness, presence of adnexal structures, chronologic aging, and photodamage. In the second case, a 45-year-old patient with a large plaque mimicking a scar or area of chronic irritation located on the upper arm was examined (Fig. 1B), with scans taken from within the tumor and 1.5 cm from the clinical

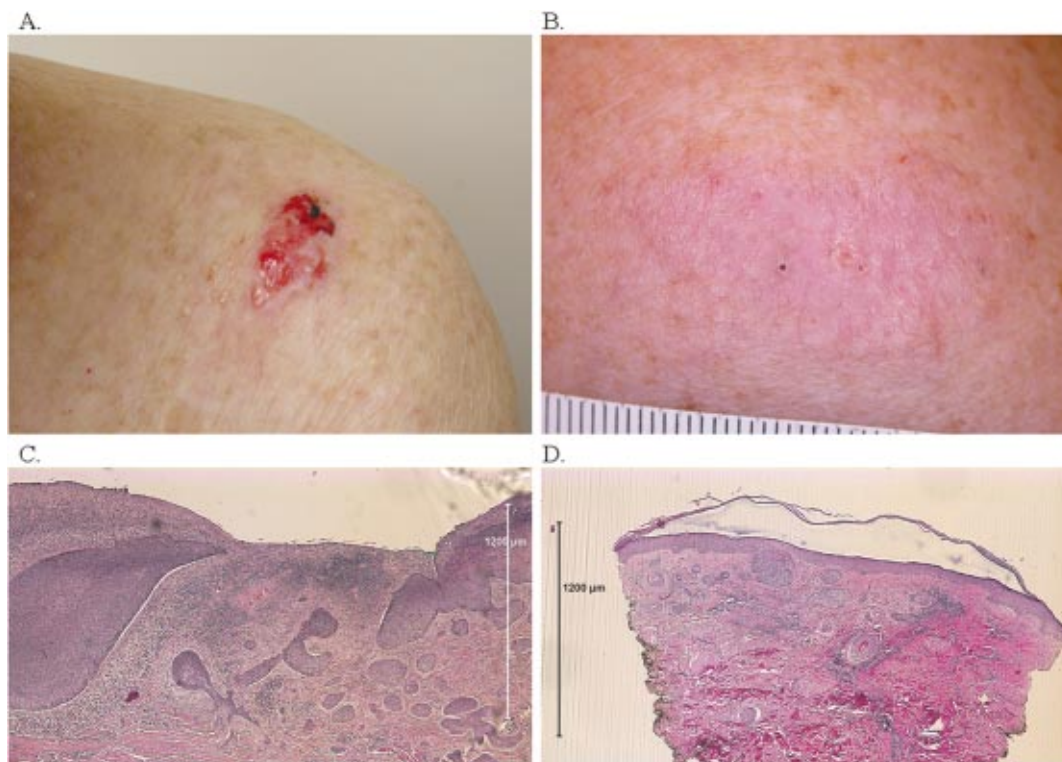


Fig. 1 Clinical and histopathologic appearance of two types of BCCs used in this study. (A) Nodular and infiltrative 3.5 cm BCC located on the upper back. (B) Infiltrative BCC, 3.0 cm, located on the shoulder. (C and D) Hematoxylin and eosin (H & E) stained histologic specimens from (A) and (B), respectively (4 \times).

tumor margin. This BCC was of the infiltrative type, characterized by smaller islands intermingling with the normal dermis, not replacing it (Fig. 1D). All areas were scanned at least five times and representative unaltered intensity OCT and PS-OCT images of both tumors are displayed in Figs. 2–4.

The intensity images are processed into an image ranging from white (weak backscattering) to black (strong backscattering) on a 256-point gray scale. Therefore a light color represents an area lacking significant backscattering structure when compared to adjacent tissue. For example, in Fig. 2A, the epidermis is therefore displayed as a light gray color; the same light color is obtained in areas where very low amounts of signal have penetrated, such as the base of the reticular dermis at the bottom of the image.

In the birefringence images, the value of the phase retardation is displayed on a separate gray scale. If the image contains birefringent material, this will cause an alteration in the polarization state, quantified as a phase retardation. One should not interpret these images in absolute terms of color (black or white); rather the *change* from black to white or vice versa as the marker of birefringence. In highly birefringent materials, there will be a strong sudden change. Three parameters may be examined as illustrated in this study. First, the location of the transition (upper or lower dermis, for example) is noted. Second, the rate of this transition viewed: black to white is quantitatively more birefringent than black to gray change. Third, one assesses whether this layer of birefringence occurs at the same depth of the skin or if it is more haphazard. Of note, areas located deep to birefringent structure may appear “scrambled gray” with a mixed collection of

pixels, indicating the photons have lost their polarization state and can no longer provide useful information about that area. Alternatively, this scattered pattern occurs in areas with very low light signal.

On the structural OCT for the first case, we identify normal skin architecture (Fig. 2A). The OCT intensity image reveals a thin epidermis (E) with faint OCT signal. This is characteristic of the thin sun-damaged skin on this patient. Deep to this is a highly backscattering (i.e., very black) papillary dermis (PD) overlying a reticular dermis (RD) containing a variety of structures, many of which do not backscatter significantly (i.e., they appear white). At the junction of the PD and the RD, one can appreciate fine, horizontally oriented structures in a regular arrangement, which have very-low-backscattering qualities. These likely represent the cutaneous superficial vascular plexus vessels (V). Deeper is a mixture of low- and high-backscattering structure with a progressively lower signal as one examines the deepest portion of the image (i.e., images become very light at the bottom of the scan).

On the corresponding birefringence image from PS-OCT (Fig. 2C), one notes that light enters the epidermis with an arbitrary polarization state displayed as black. At the mid-depth of this scan, there is an abrupt transition to white, indicating the presence of birefringent material (B). This birefringence signal coincides with the location of the reticular dermis. Deeper, there is a scrambling of the PS-OCT signal (“Scr”), which occurs at approximately the same horizontal level throughout the 5 mm scanned area.

PS-OCT images taken from the central portion of the tumor illustrate several changes. On the intensity image the first

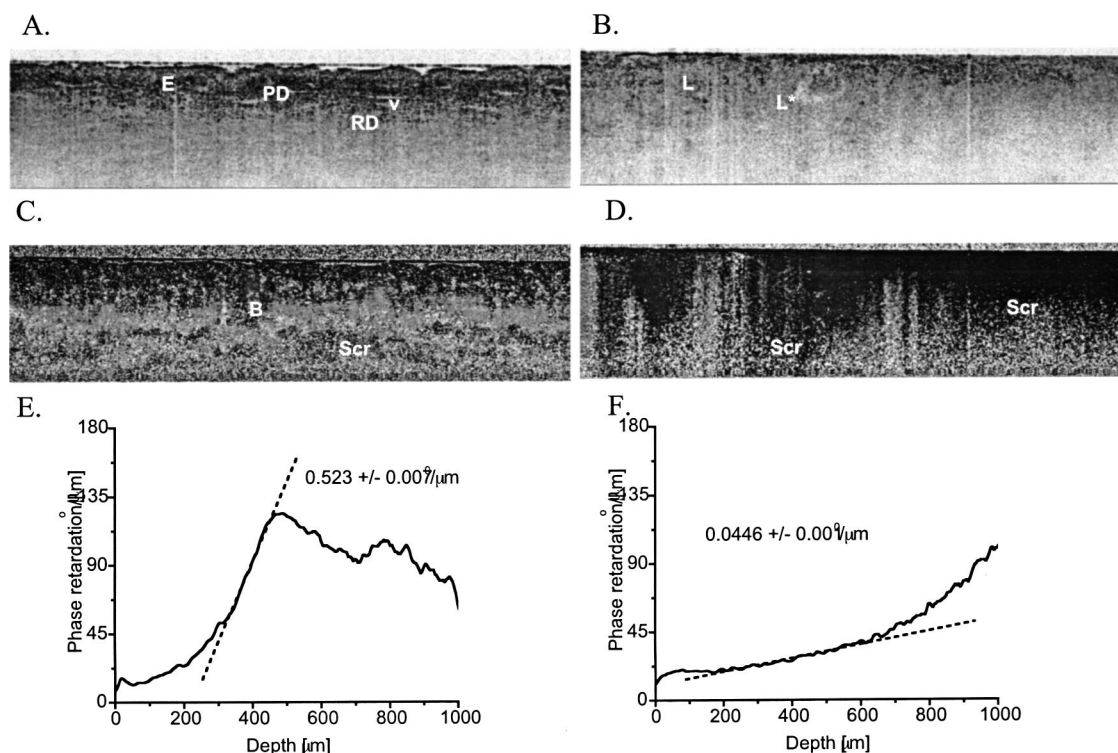


Fig. 2 Dual-mode imaging of basal cell carcinoma, nodular type with ulceration. (A) Standard intensity OCT image of uninvolved perilesional skin with intact epidermis ("E"), papillary dermis ("PD"), containing horizontally aligned vessels ("V") on a strongly backscattering (dark) background, and a gradual transition to reticular dermis ("RD"). (C) Polarization-sensitive image of the birefringent nature of the same exact frame, demonstrating a strong birefringent area, "B", indicated by the phase retardation occurring at a consistent layer of the reticular dermis, persisting for a large portion of the depth of the "RD" before becoming scrambled ("Scr"). (B) Standard intensity OCT image of a nodular infiltrative basal cell carcinoma (BCC), with loss of the normal architectural features identified in (A). There is the faint appearance of several structures measuring several hundred microns reminiscent of the lobules observed in standard histology of nodular BCC (L). These occasionally contain a rim of very-low-backscattering material (L*). (D) Polarization-sensitive image of the same tumor scan, illustrating a loss of the birefringent band of the RD, and a rapid transition to scrambled polarization signal. (E) Quantitative graph of the birefringence signals from (B). The mean phase retardation and intensity as a function of depth for perilesional skin is plotted. The gradient of a linear least-squares fit to the phase retardation data is shown. The slope is indicated. (F) Quantitative graph of the birefringence signals from (D). Mean phase retardation and intensity as a function of depth for tumor. The gradient of a linear least-squares fit to the phase retardation data is shown. The slope is indicated.

alteration is a loss of the normal arrangement of the three layers: epidermis, papillary dermis, and reticular dermis (Fig. 2B). Second, there was an absence of the horizontally oriented low-scattering structures (likely representing the vessels of the superficial vascular plexus). Third, the rapid attenuation of signal noted at the bottom of the scan is not present. In its place, one can appreciate numerous faint lobular structures (L) in the upper portion of the image. The structures appear to have a low-backscattering property surrounding a higher-scattering core (i.e., a darker core surrounded by a light-colored thin ring). Such shapes were not observed in uninvolved skin. Occasionally, one observes lobular structures with a very light backscattering ring (L*). There is less signal attenuation. The PS-OCT image reveals a loss of birefringence within the tumor itself (Fig. 2D). At the deeper portion of the image, one observes scrambled signal only ("Scr"). PS-OCT did not identify the deep tumor margin.

With the preliminary features observed for this type of tumor, we then investigated an aggressive tumor with histological features quite distinct from the ulcerated nodular tumor. Figure 3 contains the OCT and PS-OCT images of normal perilesional skin and of an infiltrative BCC. This tumor is comprised of smaller lobules that infiltrate deeply within the

dermis, leaving the overlying epidermis partially intact. Similarly to the first case presented, there is epidermal and dermal structure apparent on the intensity OCT image and a band of birefringence apparent on the intensity OCT image and a band of birefringence signal detected at mid-depth by PS-OCT (Figs. 3A, 3C). In the case of this tumor, one again appreciates loss of the normal structural skin features, with the appearance of faint lobular structures (Fig. 3B). There were no bright backscattering lobules (L* in Fig. 2B) in this tumor, however. In the PS-OCT image, there was a dramatic alteration in the birefringence signal. Normal skin has a strong uniform band at the level of the upper reticular dermis, with scrambled signal located immediately below it (Fig. 3C). This tumor contained a lower overall amount of birefringent material within the region of the scan (Fig. 3D). In contrast to the nearly absent birefringence of the ulcerated nodular BCC, this infiltrative tumor produced a more haphazard birefringent signal. The transitions from black to white occurred at various levels of the skin. In places, there was a "gap" apparent between the birefringence band and the deeper scrambled signal.

The above results are based on qualitative assessments. We applied a quantitative method to determine the amount of birefringence in each area.⁹ By plotting the mean phase shift as a function of depth across the entire image, a curve is gener-

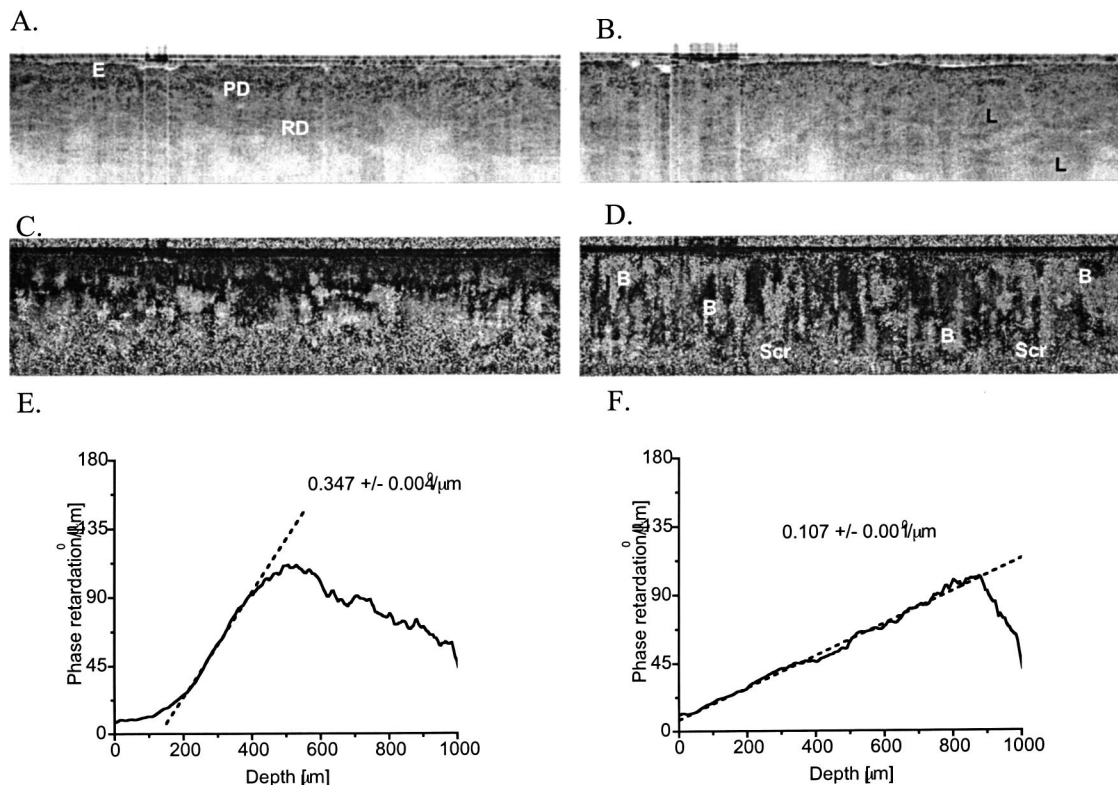


Fig. 3 Dual-mode imaging of basal cell carcinoma, infiltrative type, nonulcerated. (A) Standard intensity OCT image of uninvolved perilesional skin. Similar features are identified as discussed in Fig. 2. (C) Polarization-sensitive image of the birefringent nature of the same exact frame, demonstrating a strong birefringent area, “B”, indicated by the phase retardation occurring at a consistent layer of the reticular dermis, persisting for a large portion of the depth of the RD before becoming scrambled (Scr). (B) Standard intensity OCT image of a nodular basal cell carcinoma (BCC), with alteration of the normal architectural features identified in (A) and several lobular structures (L). (D) Polarization-sensitive image of the same tumor frame, illustrating a loss of the birefringent band of the RD, and the onset of birefringence at variable depths of the tumor, producing a less orderly appearance and a scrambled signal at the lowest portion of the image. (E) Quantitative graph of the birefringence signals from (C). The mean phase retardation and intensity as a function of depth for perilesional skin is plotted. The gradient of a linear least-squares fit to the phase retardation data is shown. The slope is indicated. (F) Quantitative graph of the birefringence signals from (D). Mean phase retardation and intensity as a function of depth for tumor. The gradient of a linear least-squares fit to the phase retardation data is shown. The slope is indicated.

ated, the slope of the which corresponds to the degree of phase shift over a given distance. In the case of normal skin, the slope is 0.52 (Fig. 2E). In contrast, the tumor demonstrates very little birefringence, with a slope of 0.04 (Fig. 2F). In the case of the infiltrative BCC, the values for perilesional skin and tumor were 0.34 (Fig. 3E), and 0.10 (Fig. 3F), respectively.

The above results suggest that PS-OCT may aid to distinguish tumor from normal skin. We therefore examined a tumor border region. Figure 4 demonstrates a scan across the visible edge. The scan is oriented such that the left portion of the image corresponds to the more normal skin and the right to more malignant skin. Thus, the former retains more characteristics of normal skin, while the latter demonstrates features more similar to tumor. Following the transition to the right, there is an alteration of the normal structure and a more homogeneous, low-backscattering area, representing tumor. In addition, this border region contained several serpiginous horizontally oriented low-backscattering structures, which may represent ectatic vessels (Fig. 4, V), a common clinical feature of all types of basal cell carcinoma. In contrast to the vessel-like structures seen in normal skin, these appear to be larger. It is not clear if these represent blood or lymphatic

vessels. In this noninvasive study, it was not possible to correlate exact features of OCT and histology to determine the precise lateral tumor extension.

4 Discussion

In this pilot study, we describe for the first time the appearance of BCC tumors when examined by PS-OCT *in vivo*. PS-OCT identified normal skin structure, including dermal birefringence. The tumors have a loss of the normal structure of skin and gain a different appearance with the impression of lobular quality to the tissue, though the exact structure that forms this is not clear. There is a dramatic alteration in birefringence in the case of both ulcerated and infiltrative examples of BCC when they are compared to each other and to perilesional skin.

OCT provides a potentially useful method to examine human skin cancers, and BCC in particular. The OCT system described here is suitable for a clinician, as it allows *in vivo* noninvasive examination of lesions using a simple fiber optic handpiece. No patient described any discomfort and we examined lesions in all portions of the body with ease. The information is presented in real time to the physician and to

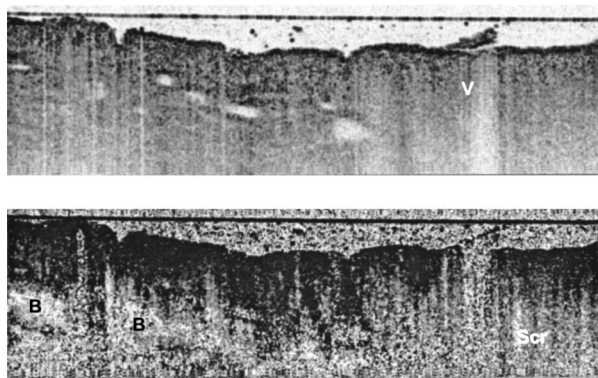


Fig. 4 Dual-mode imaging of the border transition area of basal cell carcinoma, nodular and infiltrative type. Upper frame: intensity OCT image acquired from a scan across the clinical border of a tumor, with the frank tumor located on the right. Lower frame: the birefringence image of the same scan demonstrates a characteristic strong birefringence band, B, in the mid-dermis as one approached more normal skin, and this is lost in the area of frank tumor, where it is replaced by scrambled signal (Scr).

the patient. Based on the results presented in this paper, we believe a larger case series is warranted to expand these initial observations.

We detected differences in intensity (“normal”) OCT images. There are several features of BCC that might explain this observation. First, BCC are locally invasive and destroy normal tissue architecture. OCT identified this loss of normal architecture. Second, the tumor characteristically grows in lobules; we confirmed by biopsy that these lesions also grew in a lobular pattern. Tumor lobules contain three layers: an island of tumor cells at the core, surrounded by a retraction space containing mostly mucopolysaccharides, and an outer layer of dense tumor stroma. It is likely that each of these three components will have a slightly different refractive index. OCT detects local alteration in refractive indices, and this may therefore provide the endogenous optical contrast of tumor. While there is an appearance of lobular shapes, it is possible that this does not correspond to the true tumor lobules. One possibility is that they represent a network of tumor microvessels, because the intensity of these structures is similar to that of the structures one observes at the level of the papillary/reticular dermis in a horizontal arrangement.

We anticipated that as BCC invades dermis, it would cause a loss of birefringence. This was confirmed qualitatively and quantitatively. One limitation is that the scan depth was set to 1.2 mm, so the bases of tumors were not probed, and it is unlikely that this approach will provide an *in vivo* method to detect the inferior margin of aggressive tumors. This scan depth produces reliable quality images of normal skin. The depth limitations of OCT are largely dependent on the power of the system and the optical properties of tissue. In BCC, there is less signal attenuation, and we have observed good image quality to 1.5 mm; in mucosal surfaces one can obtain improved depth imaging. Nonetheless, the immediate potential utility of OCT lies in the detection of lateral margins, as tumors are usually excised the full thickness of the skin.

The two types of tumor demonstrated different losses of birefringence. This might be due to the growth patterns. These

examples represent two ends of a spectrum of BCC histological types. On the one hand, the nodular type of growth often replaced the dermis completely, resulting in an ulcerated lesion, while the infiltrative type leaves much of the dermis intact, as well as some epidermal material. Interestingly, there is a new birefringence pattern observed in the infiltrative BCC. The birefringence was decreased but not eliminated, and the changes occurred over very short distances. It is likely a phenomenon of material at the periphery of individual tumor lobules.

The substance responsible for the increased birefringence is not clear. As sclerotic BCC induces a denser stroma, one might expect a higher local birefringence due to this collagen deposition. A second possible explanation is the birefringent material amyloid. Amyloid in skin tumors is thought to be derived from keratin and adopts the characteristic beta-sheet folding pattern to remain highly organized. It was detected in 40% of BCC in one series.¹³ Future studies should examine the presence of amyloid in the cases where we detect an altered birefringence pattern. This is certainly an avenue to exploit for possible diagnostic significance, as amyloid is more commonly associated with nodular types, and is less present in the very aggressive morpheaform BCC subtype. A third possible candidate is dystrophic calcification, which occurs in approximately 20% of basal cell carcinomas.¹⁴ This is a phenomenon whereby damaged tissue undergoes alterations resulting in the accumulation of varying amounts of calcium. Certain crystals of calcium are birefringent, though tumor-associated dystrophic calcinosis usually results in calcium hydroxyapatite crystals, usually not associated with birefringence in histologic sections.¹⁵ It possible that the ability to detect small quantities of birefringent material may vary greatly from our optical method to the conventional histopathological methods.

BCCs are most readily treated by surgical excision. We selected two tumor types that pose a challenge to the surgeon. In the case of clinically well-demarcated small tumors, a surgical margin of 3–4 mm is sufficient to clear 95% of tumors. For the types used in this study, such margins are usually insufficient as the subclinical extension of tumor can be extensive. Mohs micrographic surgery is the best modality to ensure complete removal of aggressive tumors with minimal loss of normal perilesional skin. However, the procedure is time consuming, expensive, and is performed only by specially trained cutaneous surgeons. A noninvasive, real-time optical method to detect lateral tumor margins would provide a significant aid in surgical planning. This paper describes, for the first time, OCT features of the two aggressive types of basal cell carcinoma. By using the altered intensity image appearance and altered birefringence, there is a potential for PS-OCT to serve as a tool to guide surgery of these tumors.

We anticipate that the findings observed here may also occur with other invasive cutaneous tumors, including squamous cell carcinoma and cutaneous melanoma. Future studies will address the role of PS-OCT in these tumors.

Acknowledgments

Dr. Strasswimmer received a Cutting Edge Research Grant from the American Society of Dermatologic Surgery and an

NIH NRSA (T32) Dermatology Award. Dr. de Boer received grants from the Whitaker Foundation (26083) and the Department of Defense (F4 9620-01-0014).

References

1. S. J. Miller, "Biology of basal cell carcinoma (Part I)," *J. Am. Acad. Dermatol.* **24**(1), 1–13 (1991).
2. E. B. Russell, P. R. Carrington, and B. R. Smoller, "Basal cell carcinoma: A comparison of shave biopsy versus punch biopsy techniques in subtype diagnosis," *J. Am. Acad. Dermatol.* **41**(1), 69–71 (1999).
3. C. C. Harland et al., "Differentiation of common benign pigmented skin lesions from melanoma by high-resolution ultrasound," *Br. J. Dermatol.*, **143**(2), 281–289 (2000).
4. R. M. Woodward et al., "Terahertz pulse imaging of *ex vivo* basal cell carcinoma," *J. Invest. Dermatol.* **120**(1), 72–78 (2003).
5. A. Glaessl et al., "Laser surgical planning with magnetic resonance imaging-based 3-dimensional reconstructions for intralesional Nd:YAG laser therapy of a venous malformation of the neck," *Arch. Dermatol.* **137**(10), 1331–1335 (2001).
6. S. Gonzalez and Z. Tannous, "Real-time, *in vivo* confocal reflectance microscopy of basal cell carcinoma," *J. Am. Acad. Dermatol.* **47**(6), 869–874 (2002).
7. J. S. Nelson et al., "Imaging blood flow in human port-wine stain *in situ* and in real time using optical Doppler tomography," *Arch. Dermatol.* **137**(6), 741–744 (2001).
8. J. F. de Boer and T. E. Milner, "Review of polarization sensitive optical coherence tomography and Stokes vector determination," *J. Biomed. Opt.* **7**(3), 359–371 (2002).
9. B. H. Park, C. Saxer, S. M. Srinivas, J. S. Nelson, and J. F. de Boer, "*In vivo* burn depth determination by high-speed fiber-based polarization sensitive optical coherence tomography," *J. Biomed. Opt.* **6**(4), 474–479 (2001).
10. J. Welzel et al., "Optical coherence tomography of the human skin," *J. Am. Acad. Dermatol.* **37**(6), 958–963 (1997).
11. I. F. Orenge et al., "Correlation of histologic subtypes of primary basal cell carcinoma and number of Mohs stages required to achieve a tumor-free plane," *J. Am. Acad. Dermatol.* **37**(3 Pt 1), 395–397 (1997).
12. J. J. Rippey, "Why classify basal cell carcinomas?" *Histopathology* **32**(5), 393–398 (1998).
13. L. M. Looi, "Localized amyloidosis in basal cell carcinoma: a pathologic study," *Cancer* **52**(10), 1833–1836 (1983).
14. J. S. Walsh, C. Perniciaro, and H. W. Randle, "Calcifying basal cell carcinomas," *Dermatol. Surg.* **25**(1), 49–51 (1999).
15. V. Shidham et al., "Evaluation of crystals in formalin-fixed, paraffin-embedded tissue sections for the differential diagnosis of pseudogout, gout, and tumoral calcinosis," *Mod. Pathol.* **14**(8), 806–810 (2001).
16. M. C. Pierce, B. H. Park, B. Cense, and J. F. de Boer, "Simultaneous intensity, birefringence, and flow measurements with high-speed fiber based optical coherence tomography," *Opt. Lett.* **27**(17), 1534–1536 (2002).
17. M. C. Pierce, J. Strasswimmer, B. H. Park, B. Cense, and J. F. de Boer, "Birefringence measurements in human skin using polarization-sensitive optical coherence tomography," *J. Biomed. Opt.* **9**(2) 287–291 (2004) (this issue).